TDK-dolgozat

Hock Ádám

University of Szeged
Institute of Informatics
Department of Technical Informatics

The effects of acceleration measurement parameters on determining human locomotor activity

Made by:
Ádám Hock
IV. collage year Electrical Engineering BSc

Supervisors:
Dr. Gergely Vadai
Assistant professor

Bálint Maczák
PhD student

Magyar absztrakt

Az aktigráfia módszertana több évtizedes múltra tekint vissza, aminek segítségével noninvazív módon lehet mérni az egyén motorikus aktivitását. Ehhez úgynevezett aktigráfot használnak, mely tipikusan a csuklóra helyezve méri annak háromtengelyi gyorsulását. Klasszikusan ebből csak percenként egy aktivitást jellemző mérőszámot állítanak elő és tárolnak el, viszont manapság a modernebb eszközök már magukat a gyorsulás adatokat is képesek eltárolni. Az aktigráfiás mérések elemzésével és hasznosításával számos tudományág is foglalkozik, mint például az alváskutatás vagy a pszichiátria. Mindezek ellenére a módszertan nincs standardizálva, erősen eszköz- és gyártóspecifikus az, hogy a gyorsulásadatokból hogyan számítják ki az aktivitást. Eltérések adódhatnak abból, hogy a nyers gyorsulásjelek milyen előfeldolgozásokon esnek át, mint például a jelek szűrése vagy normalizálása, másrészt abból, hogy az előfeldolgozott gyorsulás adatból milyen aktivitásmetrikával számítják ki az adott időszeletet jellemző aktivitásértéket, melyek erősen megnehezítik a tudományos munkák összevetését és reprodukálhatóságát.

A kutatócsoport, melyhez csatlakoztam, ennek a problémának a feltárásával is foglalkozik, összehasonlítva a legelterjedtebb előfeldolgozások és aktivitásmetrikák kombinációjából számított aktivitásjeleket. Korábbi korrelációs analízisük azt mutatta, hogy az eltérő aktivitásszámolási módszerek jelentős különbségeket idézhetnek elő. Munkám során még egyet léptem hátra a folyamatban, és megvizsgáltam, hogy mekkora eltéréseket okozhatnak a gyorsulásadatok méréstechnikai paraméterei az aktivitásadatok szintjén. Alváskutatókkal történő együttműködésünk mentén elemzésemet GENEActiv aktigráfokkal, 100 Hz-es mintavételi frekvencia és 12 bites felbontás mellett rögzített gyorsulásjeleken végeztem. A mintavételi ráta hatásának vizsgálatához az adatokat utólag alulmintavételeztem, ügyelve a lehetséges aliasing effektusra. Emellett felbontásukat is csökkentettem, továbbá a kutatócsoport korábban publikált módszerét felhasználva utólag kalibráltam, majd ezekből eltérő módszerekkel állítottam elő különféle aktivitásjeleket, amiket korrelációs analízissel vetettem össze, illetve időbeli és spektrális képüket is megvizsgáltam. Eredményeim alapján a méréstechnikai paraméterek módosításának elenyésző hatása van az aktivitásjelekre, ami rámutat arra, hogy a gyártói megoldások közötti lehetséges eltérések okai leginkább nem a gyorsulásmérés szintjén keresendők, hanem sokkal inkább abból erednek, hogy a különböző gyártók más aktivitásszámolási módszereket alkalmaznak eszközeikben.

English Abstract

The methodology of actigraphy has a rich past dating back several decades, making the measurement of human locomotor activity in a non-invasive manner possible. This is achieved using a device called an actigraph, which is most commonly placed on the wrist to measure acceleration along three axes. Traditionally, it only produced and stored a minute-to-minute activity value, however, several modern devices are capable of storing the raw acceleration data as well. Despite many disciplines, such as psychiatry and sleep research, being actively involved in analyzing and utilizing actigraphic measurements, the methodology is not standardized and is heavily dependent on the device and manufacturer, each calculating activity from the raw acceleration signals in varying ways. Differences can occur in the preprocessing (e.g., filtering or normalization) of the acceleration signals, as well as the type of activity metric used in the calculation of the activity value for a given time interval, making the comparability and reproducibility of scientific works especially difficult.

The research group I have joined, amongst other aspects, deals with the exploration of this problem by comparing the activity signals derived from the combinations of the most commonly used preprocessing techniques and activity metrics. Their previous correlation analysis demonstrated that the different activity determination methods can cause notable dissimilarities between activity signals. During my work, I took an additional step back in the process to investigate how certain parameters of the acceleration measurement affect the derived activity data. The measurements I examined were conducted in cooperation with sleep researchers, and were performed with GENEActiv actigraphs at a sampling rate of 100 Hz and a resolution of 12 bits. I have subsequently downsampled the data, while taking any possible aliasing effects into account. Additionally, I degraded its resolution, and calibrated it using an algorithm previously published by the group. Afterward, I calculated activity signals using several different methods, compared them by correlation analysis, and examined their temporal and spectral patterns. I found that changing the aforementioned measurement parameters has a negligible effect on the activity signals, which reinforces that possible differences between the manufacturers' solutions are not caused by the discrepancies in the technical parameters of the acceleration measurement, but rather by the different activity determination methods used in their devices

Table of contents

1. Introduction

Actigraphy is a methodology for measuring locomotor activity that is widely used in several disciplines, such as biophysics, psychiatry, and sleep research. The method is built on a special device, a so-called actigraph, which measures the acceleration in a noninvasive manner most commonly placed on the subject's wrist. The actigraph describes the locomotor activity of the subject by calculating activity values for short, consecutive, non-overlapping time intervals (i.e., epochs of typically a minute) from the measured acceleration. Traditional devices store only these activity values, but modern devices can store the raw acceleration data as well.

Despite their widespread use, the methodology of actigraphy is not standardized and the activity calculation procedures can widely differ between manufacturers based on how the acceleration data is preprocessed (e.g., digital filtering or normalizing), and the kind of activity metric (which is typically set of nonlinear operations) utilized to calculate the activity values for each epoch. Unfortunately, manufacturers rarely disclose the exact steps they take during this process, and many scientific papers do not describe the details of how they determined the activity signals, making the comparability and reproducibility of scientific works especially difficult.

I have joined a research group that, among other aspects, is trying to bring light to this problem. In the past, they have collected the mostly used activity determination methods to compare their outcomes through extensive spectral and correlational analysis. They concluded that the way activity values are derived can cause notable dissimilarities between activity signals. Since modern actigraphs contain very similar digital accelerometers of MEMS (micro-electromechanical systems) technology, and due to the specific nature of human movement, the research group suspected, that the methodological discrepancies are less likely related to the technical aspects of acceleration measurements but instead to the manufacturer-dependent activity determination procedures.

My goal was to prove this by taking a step back in the process. Using a dataset of raw actigraphic acceleration recordings, I have subsequently changed several of the acceleration measurement parameters (e.g., sampling frequency and resolution), and compared the temporal and spectral natures of the acceleration data and the resulting activity signals derived by numerous activity determination methods. Building upon the previous correlation-based analysis of the research group, I have assessed how the linear relationship between the differently calculated activity signals is affected by changing the measurement parameters. With the outcomes, I was not only able to reproduce their previous results on a different dataset, but also prove that the acceleration measurement techniques have negligible effects on the activity signals compared to the impact of the different activity determination methods. In this work, I will present these results in detail, and how I was able to make these observations.

2. Literature overview

In this section, I detail the most important mathematical concepts used throughout my analysis, the basics of actigraphy and its principle of operation, as well as the fields it is utilized in. In addition, I also cover the inconsistencies within the methodology, the problems caused by them and how I, and the research group I am a part of tries to tackle this issue.

2.1. Related techniques of activity data comparison

2.1.1. Correlation coefficient

One of the most commonly used correlational metrics is the Pearson correlation coefficient [1,2], which describes the linear relationship between two variables. It is a number within the [-1, 1] interval and is usually symbolized with *r*. It is a symmetric measure, its sign indicating the direction of the linear connection, meaning, that if *r* is positive, then as one variable increases in value the other also increases, otherwise if *r* is negative, as one variable increases in value the other decreases. The higher its absolute value, the higher the linear relationship between the variables. Let's say the two signals under study are $X = x_1, \ldots, x_n$ and $Y = y_1, \ldots, y_n$ each consisting of *n* samples. Let $\bar{x}$ and $\bar{y}$ be their averages and (x_1, y_1) ... (x_n, y_n) be the pairs made from the sample. In this case, the Pearson correlation coefficient is defined by the following equation:

$$r = \frac{\sum_{i=1}^{n}(x_i - \bar{x})\,(y_i - \bar{y})}{\sqrt{\sum_{i=1}^{n}(x_i - \bar{x})^{\,2}\,\sum_{i=1}^{n}(y_i - \bar{y})^2}} \tag{2.1}$$

The value of the coefficient can be interpreted in a variety of ways, the following table demonstrating on of them.

$\lvert\boldsymbol{r}\rvert$	Meaning
0.00–0.09	Negligible correlation
0.10-0.39	Weak correlation
0.40-0.69	Moderate correlation
0.70-0.89	Strong correlation
0.90-1.00	Very strong correlation

Table 2.1.: A possible interpretation of the Pearson correlation coefficient [2].

2.1.2. Power Spectral Density

Power spectral density (PSD) [3] describes the distribution of power between $[f_1, f_2]$ arbitrary frequencies within the examined signal. In order to calculate the power spectral density, the temporal signal must first be transformed into the frequency domain. In the case of sampled signals it is done with discrete Fourier transformation (DFT) using the following equation [4]:

$$X[k] = \sum_{n=0}^{N-1} x[n] e^{-j\frac{2\pi kn}{N}} \tag{2.2}$$

Where $k = 0, \dots, N-1$ and $x_1, \dots, x_n$ are the N samples that are to be transformed within a T long time period of the temporal signal. The result of the DFT is X, which is a vector made up of complex numbers, each element carrying a pair of vital information, being the amplitude and phase of the frequency component that corresponds to them. At this stage, X vector is two-sided, meaning that the second half of the vector (other than the 0. element, which corresponds to the DC component) contains the conjugate of the first half, making it redundant. To get a one-sided PSD, equation 2.2 can be used [5], in which f_s is the sampling frequency of the temporal signal and $0 \leq k < N/2$.

$$PSD[k] = \begin{cases} \frac{1}{f_s N} |X[k]|^2, & k = 0 \\ \frac{2}{f_s N} |X[k]|^2, & k \neq 0 \end{cases} \tag{2.3}$$

The frequency axis of the resulting one-sided PSD will go from 0 Hz to $f_s/2$ with $\Delta f = 1/T$ steps.

2.2. Actigraphy

Actigraphy is a methodology [6–8] that has become more and more widespread over time, especially recently. The methodology uses a small device called an actigraph, which is most commonly placed on the non-dominant wrist and is able to characterize human locomotor activity. Traditionally it achieved this by measuring acceleration along the three axes (triaxial) in a non-invasive manner, then by using this data to generate an activity value for continuous non-overlapping time intervals, called epochs, and lastly storing this activity value into its memory. More modern devices store not only the activity, but the raw triaxial acceleration as well.

Actigraphic measurements are of vital importance in several disciplines, such as sports science or psychiatry. Sleep study is a specific branch of psychiatry, where professional sleep researchers are able to deduce the quality of sleep [9] or describe the circadian rhythm of the patient [10] by their activity. They can also find clues pointing to certain sleep disorders [11], or potentially even mental illnesses [12].

Since actigraphy is a widely used methodology, it should be required to be highly standardized. Despite this, multiple studies [7,13] have shown, that regardless of the discipline, its use is highly inconsistent, while others criticized [14,15] the lack of transparency in how the data can be processed, as well as not disclosing crucial information about the devices, making the comparability and reproducibility of scientific works especially difficult. The research group I have joined, amongst other aspects, is also trying to deal with the exploration of this issue by collecting and comparing the most commonly used activity determination methods [16,17]. The main cause is the sheer amount of techniques used to calculate activity from the acceleration data. Not only do different manufacturers use vastly dissimilar steps when calculating activity, but often they do not even disclose their calculation procedure publicly.

One of the most popular actigraph comes from the ActiGraph LLC. company. Previously there was no documentation that detailed the exact steps they take during their calculations, so others have tried to reverse engineer them [18], but recognizing the issue, ActiGraph have made their methods of calculating activity, or Activity Count (AC) as they call it, public [19]. While this is a step in the right direction, it does not solve the problem altogether, since the differences in preprocessing and activity metrics still persist as other manufacturers withhold relevant information.

2.3. Activity calculation methods

Despite activity calculation methods being diverse, and their details often not mentioned in documentations, all follow the same principle. Firstly, after the triaxial acceleration is collected, they are preprocessed. Next, they are cut into non-overlapping continuous epochs, and lastly some kind of metric is applied to each of the epochs to get the activity signal.

To better understand the differences between each of the preprocessing methods the research group has introduced a nomenclature [16], which I will briefly explain. Let UFXYZ be the dataset that contains the triaxial acceleration signals' components per axis, or UFX, UFY and UFZ if referred to them by their respective axis. Most devices are equipped with a band-pass filter, in order to filter out the DC component, which in this case is g, the gravitational pull of the Earth. The exact parameters and orders of the filters are not publicly available, but a study [18] was able to find out, that in one of the most frequently used devices they use a third order band-pass Butterworth digital filter, with a lower cutoff frequency of 0.25 Hz and a higher cutoff frequency of 2.5 Hz. With this, let FXYZ be the dataset that is conditioned by filtering UFXYZ, or FX, FY and FZ if referred to them by their respective axis. The other way of removing g is through normalization [20], however this can only be applied to the resulting acceleration values, so let UFM be the resultant magnitude of the acceleration values, calculated from the unfiltered components of the triaxial acceleration data using equation 2.4, and let UFNM be the normalized dataset, calculated according to equation 2.5.

$$UFM[k] = \sqrt{UFX[k]^2 + UFY[k]^2 + UFZ[k]^2} \tag{2.4}$$

$$UFNM[k] = |UFM[k] - 1g| \tag{2.5}$$

If the goal is to remove g from the resultant acceleration through filtering, that can also be done in two ways, depending on when the filtering happens. Let FMpre be the dataset, that is the result of filtering the triaxial data before calculating their resultant, as shown in equation 2.6 and let FMpost be the dataset, that is the result of applying the filter after calculating the resulting acceleration.

$$FMpre[k] = \sqrt{FX[k]^2 + FY[k]^2 + FZ[k]^2} \tag{2.6}$$

These are the six preprocessing techniques I will be using throughout my analysis. A quick summary of them can be seen below:

- UFXYZ: Unfiltered components of the triaxial acceleration signal per axis
- FXYZ: Filtered components of the triaxial acceleration signal per axis
- UFM: The resultant acceleration calculated from UFXYZ
- UFNM: The resultant acceleration after normalization
- FMpre: The resultant acceleration calculated from FXYZ
- FMpost: UFM after filtering

The second step after the preprocessings, the datasets are cut into epochs. While epoch lengths can vary, they are most commonly 60 seconds long [15], which was also adapted in the research group's previous work, therefore, so I can compare my results to theirs I also used minute long epochs during my work.

The last step is to get the activity signal. This is done by applying an activity metric on each of the epochs. An activity metric defines the way the activity value is calculated from the preprocessed values within the given epoch. Several activity metrics are widely used in the literature, with each device implementing dissimilar metrics. Below is a table of 7 significantly different activity metrics, as well as their brief descriptions.

Metric Name	Brief description
Proportional Integration Method (PIM)	Determines the numerical integrate (the sum in case of discrete signals) of the acceleration values within the epoch: $$PIM = T_s \sum_{i=1}^{n} x_i$$ Where $x_1, \dots, x_n$ are the *n* acceleration values within the given epoch and T_s is the time difference between two consecutive values.
Zero Crossing Method (ZCM)	Determines the number of times the acceleration values crossed a T_{ZCM} threshold within the given epoch. In prior works of the research group [16] this threshold was established as the standard deviation of the values in the epoch.
Time Above Threshold (TAT)	Determines the number of acceleration values that were higher than a T_{TAT} threshold within the given epoch. In prior works of the research group [16] this threshold was established as the standard deviation of the values in the epoch.
Mean Amplitude Deviation (MAD)	$$MAD = \frac{1}{n} \sum_{i=1}^{n} \lvert r_i - \bar{r} \rvert$$ Where $r_1, \dots, r_n$ are the *n* acceleration values within the given epoch and $\bar{r}$ is their numerical average.
Euclidean Norm Minus One (ENMO)	$$ENMO = \frac{1}{n} \sum_{i=1}^{n} \max\,(r_i - 1, 0)$$ Where $r_1, \dots, r_n$ are the *n* acceleration values within the given epoch, whose unit of measure is *g*.
High-Pass Filtered Euclidean (HFEN)	$$HFEN = \frac{1}{n} \sum_{i=1}^{n} r_{fi}$$ Where $r_1, \dots, r_n$ are the *n* specially filtered, resultant acceleration values within the given epoch. In this case, unlike any of the previously mentioned preprocessing methods, the per-axis acceleration values are filtered by a high-pass filter, before calculating their r_{fi} resultant acceleration.

Activity Index (AI)	$$AI = \sqrt{\max\left(\frac{1}{3}\left(\sum_{m=1}^{3}\sigma_m^2 - \bar{\sigma}^2\right), 0\right)}$$ Where $m = 1,2,3$ denotes the three axes, σ_m^2 is the variance of the acceleration values along the mth axis within the given epoch and $\bar{\sigma}^2$ is the variance of the noise in the entire measurement (*systematic noise variance*)
Activity Count (AC)	A complex activity metric that is used by the ActiGraph LLC. manufacturer. It utilizes several filers, and resampling techniques, as well as numerical integration. The full description is publicly available [19].

Table 2.2.: The more common activity metrics in the literature and their brief description

It is important to mention that not all activity metrics are compatible with all preprocessing methods. Figure 2.1 depicts all possible combinations.

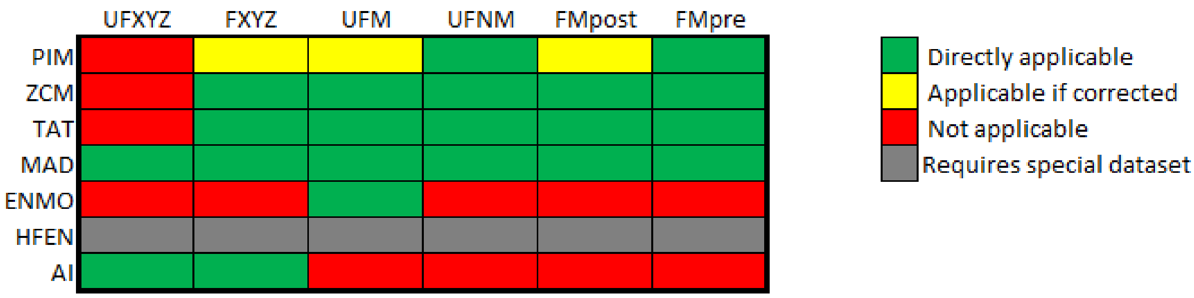

Figure 2.1: All possible preprocessing and activity metric combinations used by the research group [16,17]

In addition to these, I also calculated two additional activity signals. These were AC, which is described in Table 2.2, and VM3*, which can be calculated using Equation 2.7.

$$VM3^* = \sqrt{PIM(FX)^2 + PIM(FY)^2 + PIM(FZ)^2} \tag{2.7}$$

2.4. Differences in collecting actigraphic data

As detailed in the previous section, there are a lot of activity determination methods that differ in how they preprocess the acceleration data, as well as the activity metric they use to calculate the epoch-by-epoch activity values. This process is a lossy compression of the acceleration data, and each of the steps alters the way the compression is done. In the past, the research group did an in-depth analysis [16,17] and compared the activity signals derived by using different preprocessing techniques and activity metrics. By comparing the activity data, they found that using the same preprocessing method but applying different metrics results in strongly similar activity signals, however, they identified dissimilarities when using different preprocessing methods.

Through temporal and spectral analysis, they concluded, that while the temporal signals showed dissimilarities in some cases, most activity and acceleration signals (even the raw wrist movement) followed a universal spectral characteristic, independent of how they are determined. This raises the question of whether it is necessary to calculate activity from the acceleration data since the information content of activity signals is already present at the level of acceleration data, and since nowadays some devices are able to store the raw acceleration data making them readily available. However, there could be discrepancies in the acceleration data collection between different manufacturers' devices, because even if they use similar digital output MEMS sensors, there could be differences in the exact measurement parameters (e.g., sampling frequency, full-scale, bit resolution).

It is natural for users, especially for those who utilize these datasets for medical purposes, to be concerned with the accuracy of acceleration measurements that come from different actigraphs. Recently, several studies [15,21] have taken into consideration, how similar outcomes (e.g., sleep-wake classification) can be derived from the examination of actigraphic acceleration data measured with different hardware and found no significant differences. However, these studies do not emphasize the diversity of activity determination procedures, but rather how they can gather information from the acceleration data, which can lead to systematic misunderstandings regarding activity determination. For example, the most popular R software package that is advertised for dealing with acceleration recording, by default, converts the acceleration data into activity values in a particular way, unbeknownst to the average user, therefore, the sleep research-oriented analyses are carried out on activity data in reality. Even from that example, it is evident that the activity determination methods are an integral part of the methodology despite being lossy compressions, and they are not avoided even if the devices are able to record raw acceleration data.

2.5. Objectives

As I previously mentioned, the activity determination procedures can have a significant impact on the activity data, but the question naturally arises, that in contrast to the effects of the different compression techniques, how influential are the technical parameters of the acceleration measurement on the resulting activity data? The research group wanted to explore this question in detail, and after joining them, this has also become my objective. To answer it, I wanted to investigate the effects of subsequently calibrating real acceleration data, changing its sampling frequency from 100 Hz to 10 Hz and its bit resolution from 12 down to 4 bits. To address the impact of these modifications, I inspected the time-, and frequency-domain nature of the altered acceleration data, and explored the linear relationship between activity data derived from them by using different calculation methods with correlation analysis.

3. Materials and methods

My work was done in MATLAB, Python and LabVIEW. MATLAB provides structures that make dealing with large quantities and varying types of data easy and also allows seamless Python integration. It also has several built-in functions, like PSD and correlation calculations, which were necessary throughout my analysis. I used Python because of the several useful libraries and functions available, and because the AC calculation method was published as an open-source Python library as well [19]. I used LabVIEW, since that is the environment the research group has used in the past, therefore some programs, like the calibration method or the reading and writing of the measurement files, were readily available.

3.1. Examined data

We are in cooperation with sleep researchers at Semmelweis University, Institute of Behavioural Sciences, who conducted real measurements using a GENEActiv actigraph. The device [22] was placed on the non-dominant wrists of the individuals and has an acceleration range of $\pm$ 8 g and a resolution of 12 bits (or roughly 3.9 mg). Its sampling rate is adjustable from 10 Hz all the way to 100 Hz, and it is able to store raw triaxial acceleration data into its 0.5 Gb non-volatile flash memory.

Through our cooperation, we received a total of 28 files containing separate measurements, each containing the raw triaxial acceleration data at 100 Hz sampling frequency and spanning over the course of 7 days. From these, I was able to retrieve the stored data and subsequently modify several of the measurement parameters.

3.2. Methods of modifying measurement parameters

3.2.1. Data calibration

The calibration algorithm was done and publicized [23] by other group members prior to my joining. While devices are calibrated by their manufacturers, with time they become inaccurate due to external factors, such as temperature. The algorithm made by the group is special, since it can calibrate actigraphic measurements subsequently, after they were recorded. It detects resting periods, with little to no movement, during which the resultant acceleration should be exactly 1 g. It collects calibration points from said periods, and puts them into a three-dimensional space. Ideally, all calibration points should lie on the surface of a unit sphere centred at the origin, however, due to noise plaguing the measurement, as well as the device becoming less accurate over time, they lie on the surface of an ellipsoid instead, whose centre may not even be the origin. The algorithm then tries to transform this ellipsoid closer to a sphere throughout several iterations. As a result, it calculates 9 calibration coefficients, accounting for the deterministic scale, the non-orthogonality of the axes, as well as their offset errors. They can then easily be applied to the original acceleration values using the following equations:

$$a_x = k_{xx}(v_x + o_x) \tag{3.1}$$
$$a_y = k_{xy}(v_x + o_x) + k_{yy}(v_y + o_y) \tag{3.2}$$
$$a_z = k_{xz}(v_x + o_x) + k_{yz}(v_y + o_y) + k_{zz}(v_z + o_z) \tag{3.3}$$

Where a_x, a_y and a_z are the calibrated, v_x, v_y and v_z are the original uncalibrated acceleration values along the three axes, k_{ij} corresponds to the coefficients due to non-orthogonality, and o_k corresponds to the coefficients due to offset errors. A demonstration of the calibration algorithm between uncalibrated (blue) and calibrated (red temporal) UFM acceleration signals is shown in Figure 3.1.

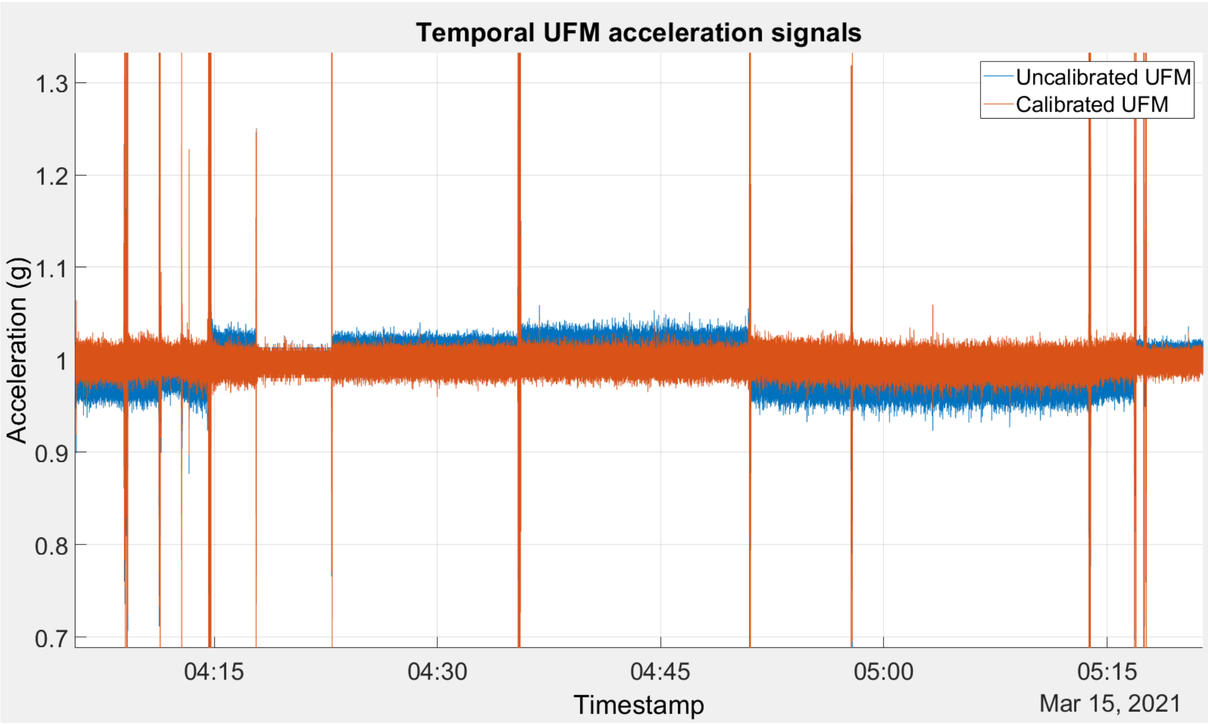

Figure 3.1: The temporal representation of the uncalibrated (blue) and calibrated (red) versions of the same UFM acceleration

3.2.2. Downsampling

Downsampling, also known as decimation, [24] in digital signal processing refers to the process of decreasing the bandwidth and sampling frequency of the original signal, thus removing certain data points from the measurement, in order to reduce data volume, or the necessary computational power, however, this can lead to an effect called aliasing. Aliasing [25] refers to overlapping frequency components due to the sampling rate not being high enough to accurately trace high frequency changes in the signal. As a result, frequencies that are not present in the original signal can appear in the PSD. To avoid aliasing, the Nyquist-Shannon sampling theorem must be adhered to, which states, that the sampling rate must greater than the half of highest frequency component in the signal (otherwise known as the Nyquist frequency). If we comply, the original signal can be fully and accurately reconstructed, however, failure to do so will result in aliasing, causing distortion and inaccuracy within the signal. It is most often unknown what the highest frequency component will be, calling for the use of anti-aliasing filters. These low-pass filters ensure, that all frequencies above the Nyquist frequency are mitigated, making the effects of aliasing negligible. The downside of these filters is that they slightly alter the data, and introduce a temporal shift as well. There are also several filter designs, each having their own benefits and downsides [26].

The original datasets of the measurements we received had a sampling frequency of a 100 Hz, which I subsequently downsampled to 10 Hz, by only keeping every 10th data point. Since this breaks the Nyquist-Shannon sampling theorem, as in this case Nyquist frequency is 50 Hz, whereas the sampling rate is only 10 Hz, I had to use an anti-aliasing filter. Chebysev filters have steep cutoffs and narrow transition bands [26,27], so I opted for the use of a low-pass Chebyshev type 1 infinite impulse response (IIR) filter of order 8, however its downside is that it causes some passband ripple. I was also curios of how strong the aliasing effect is, and whether its effect is significant, totally negligible, or somewhere in the middle. Because of this, I did the downsampling without applying any anti-aliasing filters as well, by simply keeping only every 10th point. Going forward, I will refer to these signals as O100, for the original, F10, for the downsampled dataset where an anti-aliasing filter is used, and UF10, for the downsampled dataset where no filter is used and only every 10th data point was kept.

3.2.3. Bit resolution reduction

Actigraphs contain a digital output MEMS (micro-electromechanical systems), which is the primary sensor used to measure acceleration. These contain an analogue to digital converter (ADC), which makes storing the individual data points possible. Possibly the two most important parameters of these converters is their resolution, often specified by their number of bits, and their full-scale. These two determine the set of numbers that their outputs can be. This is done by splitting the range of the converter into 2^b steps, where b is the number of bits. The difference between two consecutive values is call the quantization step, which determines the precision of the output. The precision of an ADC describes how close the digital output value can be to the original analogue value. With a set range, the higher the number of bits, the smaller the quantization steps, and the higher the precision. If the resolution is set, but the range is lowered, the quantization steps also decrease, in theory, making the output more precise. However, this is assuming that all the original data points fall into the smaller range. If that requirement is not met, it will result in loss of data due to saturation, and incorrect values. The outputs of the ADC are the values that eventually get stored into the actigraphs memory. This means, that with higher resolutions, more memory is needed to store the same amount of data points. My goal was to examine the effects of bit resolution reduction, as it could significantly decrease the memory needed for measurements, while also making the design of actigraphs much more simple and straight forward from an electronic standpoint.

The original datasets of the measurements we received had a range of $\pm 8\ g$, and a resolution of 12 bits. This means, that the quantization steps are around 3.9 mg. I have subsequently reduced the number of bits of the acceleration signals along each three of the axes from 12 to 8. I did this by first defining the new quantization step size, then rounding the 12 bit values into the nearest steps. As a result, the quantization steps became roughly 62.5 mg, This is higher than all of the publicly available devices we could find [22,28–30].

3.3. Examination techniques

Throughout my analysis I compared the acceleration data and the subsequently calculated activity signals from three different aspects, being temporal, spectral and correlational. The temporal comparison required the display of the magnitude of the acceleration as a function of their associated timestamps. For the correlational and spectral analysis I used varying processing techniques, in order to present the data in an easy to understand manner. The methods I used are discussed in the following sections.

3.3.1 Correlational

My correlational analysis is based on the Pearson correlation coefficient, detailed earlier in section 2.1.1. To be able to perceive the differences in the best way, I constructed correlational matrices. These matrices contained the correlational coefficients between the activity signals derived from the accelerations using all 37 possible preprocessing and activity metric combinations shown in Figure 2.1. Each nomenclature is depicted on both the left side, and the top of the matrix, so that it is easy to tell which cell in the matrix corresponds to the correlation coefficient between two certain combinations. I then coloured each cell depending on the absolute value of the correlation coefficient in it. The closer it is to 1, the greener the cell is, and as it decreases the cells colour shifts to yellow. This makes the comprehension of such matrices straightforward through visual representation, while also making the recognition of patterns between different matrices accessible as well. The diagonal of the matrix is highlighted, as those are the correlational values between the same activity determination techniques, and depict the exact effects the parameters have on the activity signals. An example matrix can be seen in Figure 3.2.

I made independent matrices for all 28 of the measurements. From these, I made a separate matrix which contains the averages of them, in order to make the results more generalized, so that it depicts the effects of the parameters more accurately, while also making my results easier to present. I then repeated this process each of the three adjusted parameters.

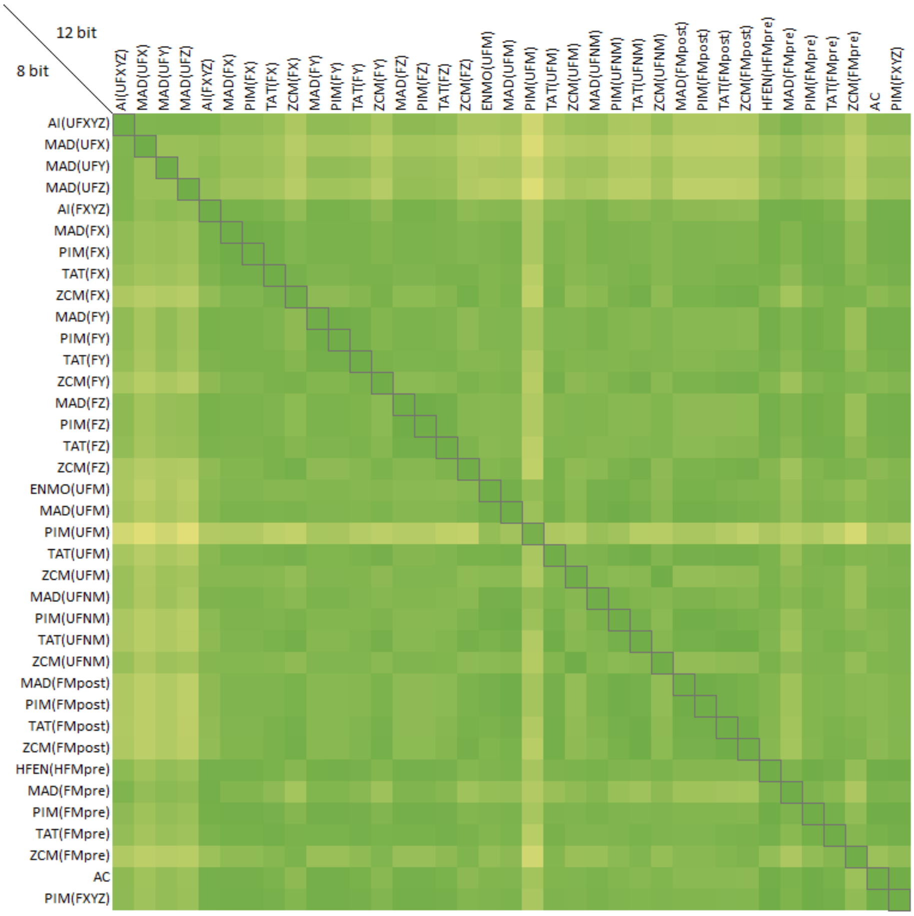

Figure 3.2: An example of a correlational matrix

3.3.2. Spectral

Other than looking at the parameters' temporal effects I also examined the spectral differences they might cause. My spectral analysis is based on the PSD of the signal, detailed earlier in section 2.1.2. The spectrum of a signal depicts the frequencies within it, as well as the total power distribution on a logarithmic scale. The understanding of spectrums can be a difficult task in the case of measurements that contain large quantities of data points, due to the sheer amount of frequencies present in the signal, further worsened by high levels of noise plaguing it, introducing even more frequency components. The research group has done spectral analysis in the past, and have used the Daniell method, detailed in their supplementary materials section [16]. To give a brief summary, the method splits the spectrum into several smaller bins per decade, each being of equal distance from one another on a logarithmic scale. Then the mean of all components in the bin is calculated and placed in the centre of the bin. While this does significantly reduce the number of points in the spectrum, it does not change the nature of it.

4. Analysis

I took an in depth look at how acceleration measurement parameters affect the temporal and spectral patterns of acceleration signals. Through correlational analysis I also assessed the linear relationship between activity signals derived by numerous activity determination methods. In each case, I calculated a correlation matrix for each of the 28 measurements, and a separate matrix containing their averages. In this section I talk about my results and conclusions for all examined parameters.

4.1. Effects of calibration

In the case of calibration, I made three separate sets of matrices. These are between the activity values derived from uncalibrated-uncalibrated, calibrated-calibrated and uncalibrated-calibrated acceleration signals. I did this, in order to find out, not only about effects of calibration, but also whether calibration modified the overall pattern and nature of these matrices, or whether they might be more potent on certain preprocesses or metrics than others. I also wanted to examine the correlation between the activity signals derived from using the same activity metric, but different preprocessing techniques and vice versa. With these matrices I was also able to validate the research group's prior works.

Firstly, I examined the matrix between the activity values calculated from uncalibrated-uncalibrated acceleration signals, shown in shown in Figure 4.1. This matrix is diagonally mirrored, since I used correlation on the same set of activity signals, which also means that their diagonal values are always exactly 1, therefore I did not highlight them this time. It can be observed that on average, the activity signals show strong correlation throughout, however, there is a noticeable shift in tone between the activities calculated from unfiltered acceleration data, and the rest. This is because the high frequency components, as well as the noises not being filtered out. It can also be observed, that the correlational value between activity signals derived from acceleration data along separate axes, as well as activity signals calculated from the magnitudes of the triaxial acceleration values are also strong. This implies, that it is rare for the wrist, where the actigraph was located, to only move along one of the three axes.

The matrix between the activity values calculated from calibrated-calibrated acceleration signals, shown in Figure 8.1 in the Supplementary Materials section, depicts an almost identical pattern. The only noticeable difference is in the PIM(UFM) activity, which is likely due to several factors. Since UFM is the unfiltered magnitude of the acceleration signals, it carries the most noise amongst all preprocessing methods, as the noises along the individual axes are accumulated when calculating the resultant. This is then worsened by the integration used during the PIM metric, adding together the noises in each and every data point. The integration also sums up the 1 *g* that is always present in the acceleration magnitude, resulting in even further inaccuracies. This activity determination method (PIM(UFM)) will in most cases be an outlier due these reasons. Other then this particular signal, there are no other glaring dissimilarities between the two matrices.

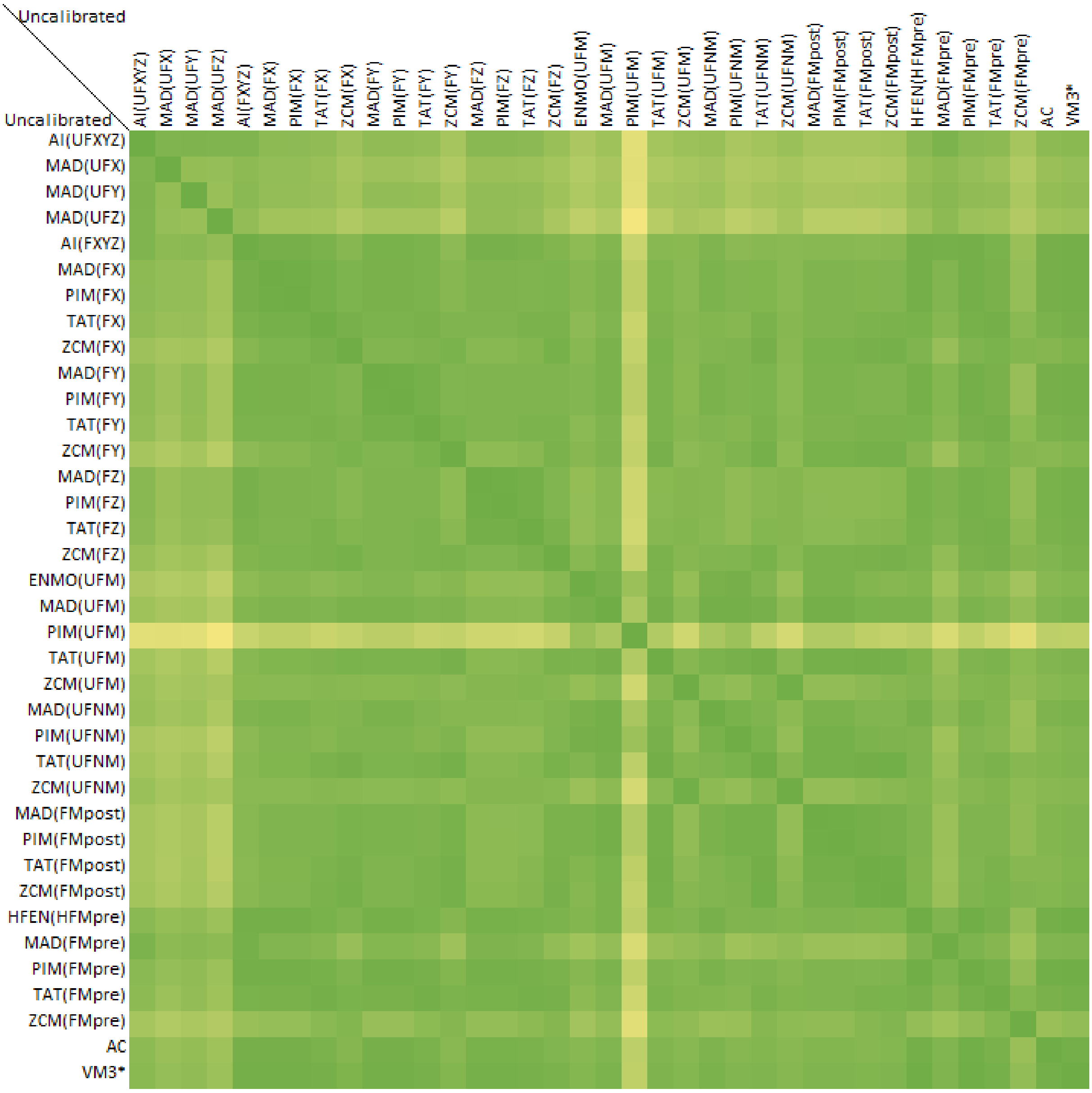

Figure 4.1: The correlational matrix between activity signals derived from uncalibrated-uncalibrated acceleration signals

I then compared my own calibrated-calibrated correlational matrix with the research group’s past conclusions. They made their matrices publicly available, and can be downloaded from their publication [16]. They did their analysis using different datasets, recorded with a completely different device. Their data was collected by an actigraph they specially made for their own project. During their data collection process, the device was also placed on the non-dominant wrists of the individuals and had a range of $\pm 8\ g$, however it only had a sampling frequency of 10 Hz. Furthermore, while the measurement datasets I examined were recorded over the course of 7 days, theirs was recorded over the course of 10. When comparing the resulting patterns between their matrices and mine, no significant changes can be observed. The overall patterns of the matrices are identical, with the only slightly different metrics being ZCM(UFM) and ZCM(UFNM). These are however likely due to the difference in sampling rates. I will explain this in more detail in the next section, that dives deeper into the effects of downsampling. What we can conclude from these results, is that despite the usage of two totally different devices, the correlation pattern of differently determined activity signals showed remarkable similarities between the two datasets, suggesting that the acceleration collection process is not dependent or specific to any certain device.

When taking a look at the matrix depicting the correlational relationship between the activity signals derived from calibrated and uncalibrated acceleration signals, shown in Figure 4.2, we can see a pattern that is naturally very similar to the previous matrices. This time around I have highlighted the diagonal of the matrix, as these are the cells carrying the most important information, as they depict the exact effects of the examined parameter separately for each activity determination procedure. I have made a separate table that contains each of the diagonal values, shown in Table 4.1. We can see, that other than PIM(UFM), all show extremely high correlation, and even that shows strong correlation. The difference is likely due to the same reasons discussed earlier. This means that calibration in the vast majority cases, has negligible effects on the different activity signal determination methods.

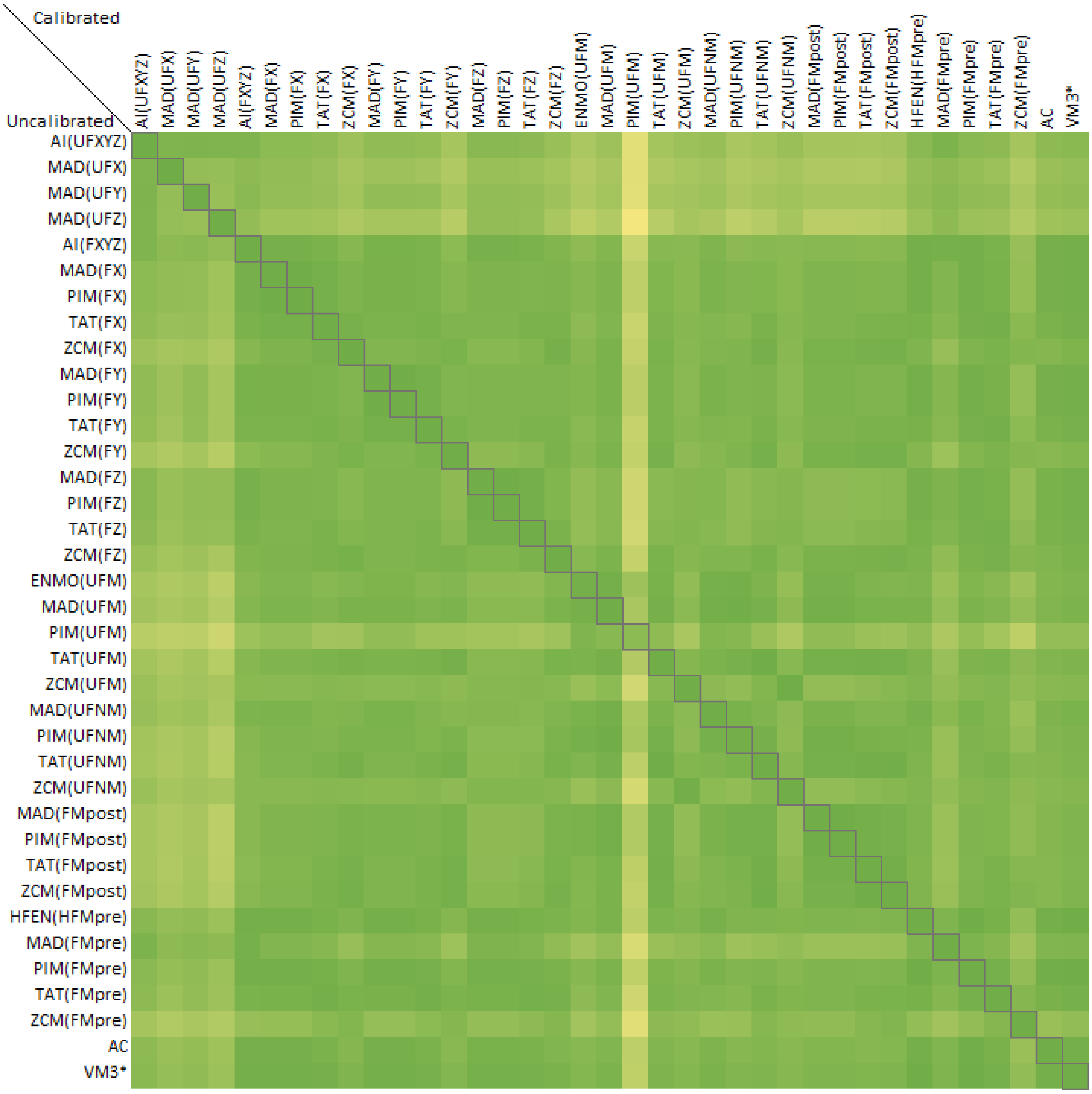

Figure 4.2: The correlational matrix between activity signals derived from uncalibrated and calibrated acceleration signals

	UFX	UFY	UFZ	FX	FY	FZ	UFM	UFNM	Fmpost	Fmpre	HFMpre
AI		1,000			1,000						
ENMO							0,971				
HFEN											1,000
MAD	1,000	1,000	1,000	1,000	1,000	1,000	0,999	0,999	1,000	1,000	
PIM				1,000	1,000	1,000	0,805	0,985	1,000	1,000	
TAT				1,000	1,000	1,000	0,998	0,999	1,000	1,000	
ZCM				1,000	1,000	1,000	0,992	0,997	0,999	1,000	
AC		1,000									
VM3*					1,000						

Table 4.1: The diagonal values in the uncalibrated-calibrated correlational matrix, where the columns are the acceleration preprocessing methods, the rows are the activity metrics, and each cell is the combination of the two containing the correlational value between the uncalibrated and calibrated activity signals

However, this does not mean that calibration is unnecessary. Its purpose is to reduce measurement errors, such as deterministic scale, non-orthogonality, and offset, of the recorded acceleration data which could be beneficial some cases of specific analyses. As seen before, on Figure 3.1, we can see that the magnitude of the uncalibrated acceleration signal is often changing around 1 *g*, sometimes slightly exceeding it, and sometimes dropping slightly below it. This is because each axis has varying levels of deterministic errors, and during resting periods when the resultant acceleration should be exactly 1 *g*, a change in the orientation of the actigraph also changes the factor of the errors that the separate axes have. Meanwhile, the calibrated acceleration signal is constantly right on the 1 *g* mark, proving that the calibration algorithm is working correctly. Despite this, it seems that its effects are small enough to diminish during the activity calculations.

4.2. Effects of sampling frequency

I will now take a deeper look into the temporal and spectral effects, as well as the changes in correlational pattern that the reduction of the sampling frequency of acceleration data induces on the activity signals derived from it. I will compare 3 different acceleration signals, being the original 100 Hz (O100) one, the 10 Hz one that takes every 10th point out from the original (UF10), and the 10 Hz one where an antialiasing-filter is used before the downsampling process (F10).

4.2.1. Temporal and spectral effects

The temporal representation of the three signals derived from the same UFM acceleration can be seen in Figure 4.3, where O100 is shown in blue, F10 is shown in red and UF10 is shown in green. When comparing F10 to O100 it can clearly be seen, that it follows its overall pattern but evens out the more rapid, higher frequency movements, which is entirely due to the anti-aliasing filter. When comparing the O100 and UF10 accelerations signals, UF10 might seem a bit unreliable, since it only keeps every 10th point of the O100, but overall, it still seems to be able to follow the patterns of it. While certain smaller spikes might be missed during the downsampling process, a study [14] depicted, that human locomotor activity rarely exceeds the 3-4 Hz range, which is not fast enough to cause meaningful changes in the patterns of the temporal acceleration signals. When comparing the F10 and UF10 acceleration signals they are often very close to one another. F10 appears to track the overall pattern of O100 a bit better, due to the somewhat random nature of UF10.

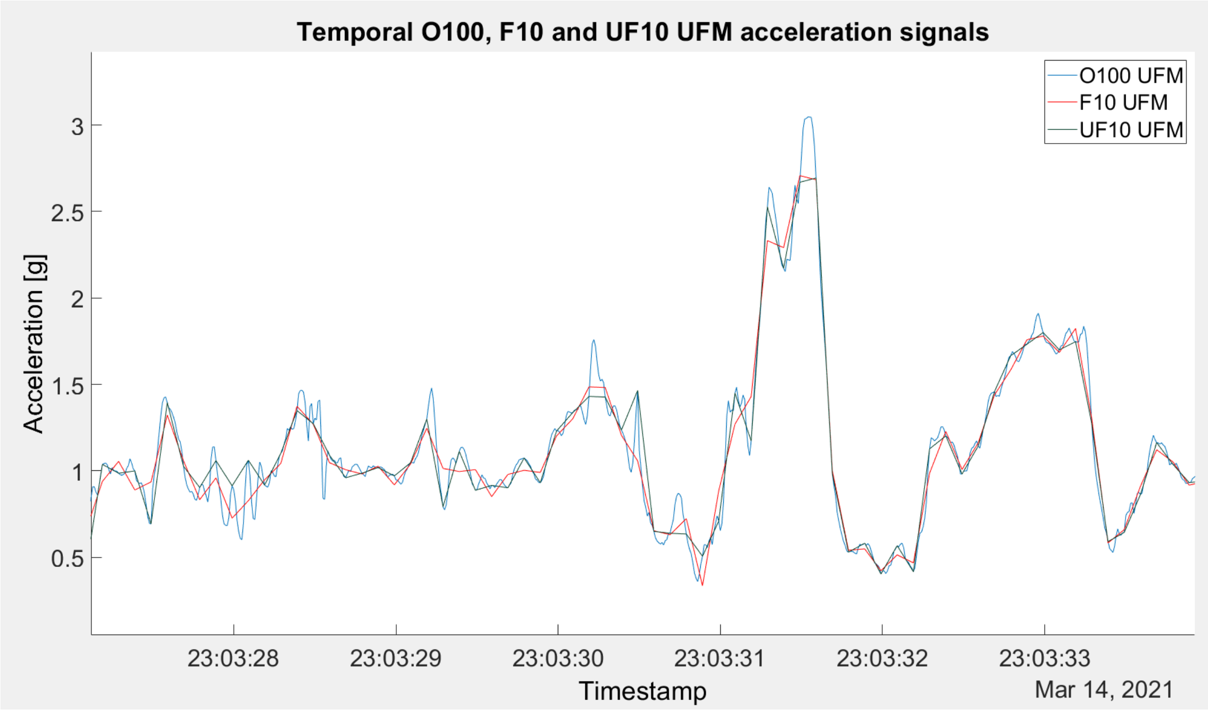

Figure 4.3: The temporal representation of the O100 (blue), F10 (red) and UF10 (green) versions of the same UFM acceleration

When looking at the binned spectrums of the signals shown in Figure 4.4, it is evident, that they are widely similar. It was to be expected, since if the temporal signals are close to each other, the spectrums must also represent that. A drop in the F10 acceleration signal at around the 3 Hz frequency mark can be clearly seen, which is caused by the anti-aliasing filter that was applied, but until that point it follows the spectrum of the O100 almost perfectly. UF10 splits slightly from the other two at the higher frequencies, however, it still follows their overall patterns. This is the aliasing effect coming into play, slightly altering the spectrum by bringing new frequencies into the signal, that were not present in the original, and as a result slightly altering the total power and its distribution. However the power at higher frequencies is negligible when compared to the total power.

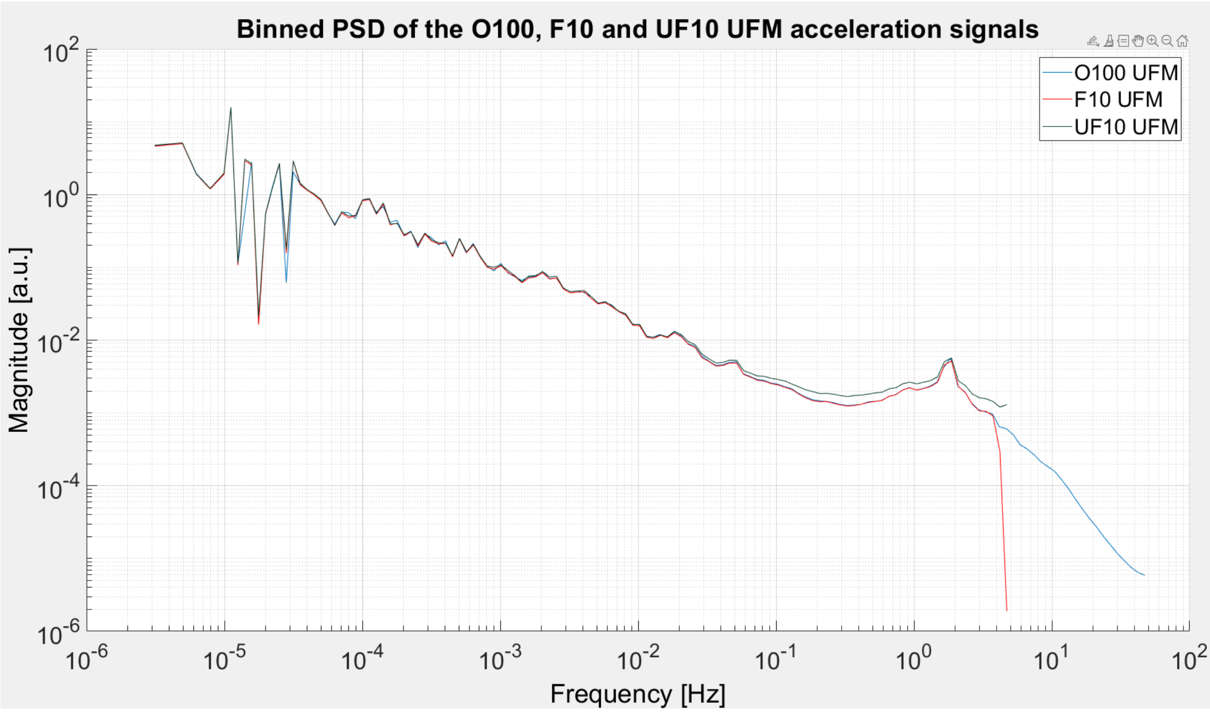

Figure 4.4: The binned power spectral density of the O100 (blue), F10 (red) and UF10 (green) versions of the same UFM acceleration

4.2.2. Correlation analysis

In order to examine all aspects and effects of the sampling frequency I made 3 separate correlational matrices here as well. These are between the sets of activity signals calculated from the UF10-O100, the F10-O100 and F10-UF10 accelerations. This way I could clearly determine the effects caused by the sampling frequency alone, as well as the aliasing effect when that is not taken into account. From the similar temporal and spectral patterns of the acceleration signals, the assumption is that the activity data calculated using different determination methods will also show strong correlations with one another.

First let's compare the activity signals calculated from the O100 and UF10 acceleration data, meaning that these are between the original acceleration signal, and the acceleration signal that only keeps every 10th data point of the prior. The correlational matrix between these two can be seen in Figure 4.5. The pattern of the correlational matrix is almost identical to the one we saw before when discussing the effects of calibration. The diagonal values of the matrix can be seen in Table 4.2. These also prove the very strong correlation between the activity signals, however a slight drop can be observed when the ZCM metric is applied, especially in the case of the UFM and UFNM preprocesses. These are because of the aliasing effect, where the UF10 signal is unable to accurately trace the higher frequency temporal movements, which results in the threshold used to calculate the ZCM metric being crossed somewhat less frequently. This is backed by the fact that the TAT metric, which also uses a threshold, showed essentially no changes. This is also the reason why, the research groups matrix showed a slightly different shade in the ZCM metric compared to mine in the previous section.

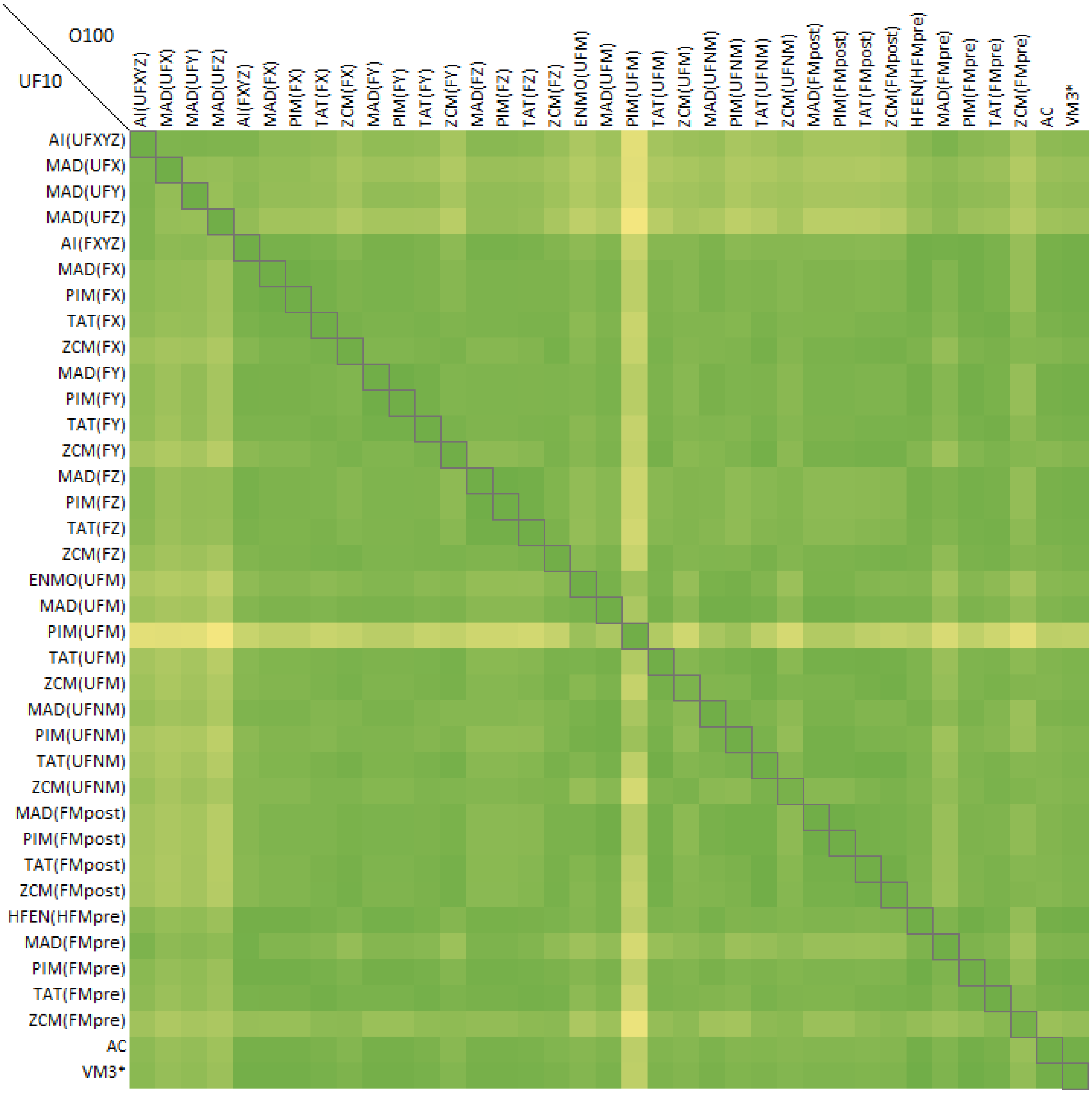

Figure 4.5: The correlational matrix between activity signals derived from the UF10 and O100 acceleration signals

	UFX	UFY	UFZ	FX	FY	FZ	UFM	UFNM	Fmpost	Fmpre	HFMpre
AI		1,000			0,996						
ENMO							0,999				
HFEN											1,000
MAD	1,000	1,000	1,000	0,994	0,998	0,997	0,999	0,999	0,994	0,996	
PIM				0,994	0,998	0,997	0,996	0,999	0,994	0,998	
TAT				0,993	0,997	0,996	0,999	0,999	0,993	0,997	
ZCM				0,988	0,993	0,991	0,916	0,938	0,991	0,957	
AC		0,998									
VM3*					0,998						

Table 4.2: The diagonal values in the UF10-O100 correlational matrix where the columns are the acceleration preprocessing methods, the rows are the activity metrics, and each cell is the combination of the two containing the correlational value between the UF10 and O100 activity signals

Second, let's take a look at the matrix containing the correlational values between the activities determined from the F10 and O100 acceleration signals. This matrix can be seen in Figure 8.2 in the Supplementary Materials section. Although, this once again shows very strong correlations throughout the entire matrix, there is a significant drop in the correlation when looking at the PIM(UFM) activity. This was to be expected, since from the temporal representation we could see, that while the F10 acceleration signal follows the overall pattern of the O100, it does smooth out the high frequency movements. As a result of those components being left out from the integration of the PIM metric, the correlational value becomes somewhat smaller, similar to how it was during the calibration process. When taking a look at the diagonal values of the matrix, shown in Table 4.3, we can see that it is similar to the previous one, however a further decrease of values can be observed in when using the ZCM metric and UFM preprocessing. This time however, it is not because of the aliasing effect, but rather because of the anti-aliasing filter. The whole purpose for implementing these filters is to get rid of the higher frequency components. With these not being present in the signal, the threshold used to calculate the ZCM metric is crossed several less number of times. This is once again reinforced by the fact that the TAT metric barely changed, and shows a correlational value of 0,99. What this means, is that the time spent above the threshold is almost identical, but because of the disappearance of the higher frequencies, it was crossed less.

	UFX	UFY	UFZ	FX	FY	FZ	UFM	UFNM	Fmpost	Fmpre	HFMpre
AI	0,998			1,000							
ENMO							0,986				
HFEN											0,996
MAD	0,998	1,000	0,999	1,000	1,000	1,000	0,989	0,988	0,997	1,000	
PIM				1,000	1,000	1,000	0,819	0,976	0,997	1,000	
TAT				0,999	0,999	0,999	0,990	0,989	0,998	1,000	
ZCM				0,993	0,997	0,996	0,863	0,903	0,995	0,969	
AC	1,000										
VM3*				1,000							

Table 4.3: The diagonal values in the F10-O100 correlational matrix where the columns are the acceleration preprocessing methods, the rows are the activity metrics, and each cell is the combination of the two containing the correlational value between the F10 and O100 activity signals

Lastly, let's compare the F10 and UF10 acceleration signals. The matrix corresponding to the correlational values between these two can be seen in Figure 8.3 in the Supplementary Materials section. This shows the same patterns as described before, with the PIM metric being the only one with lower correlation. The diagonal values are shown in Table 4.4, and are also very similar in nature to the previous ones. This has some very interesting implications. My results show, that on average, doing the downsampling the correct way, by using an anti-aliasing filter, yields slightly worse correlational values than not caring about the aliasing effect.

What this means, is that during the downsampling process, aliasing changes the activity signals less than the filter that is meant to counter it. Still, it is also important to recognize that the differences between them are very small, and neither have any meaningful effects when talking about activity signals, as all still show strong correlation with one another.

	UFX	UFY	UFZ	FX	FY	FZ	UFM	UFNM	Fmpost	Fmpre	HFMpre
AI		0,998			0,996						
ENMO							0,985				
HFEN											0,996
MAD	0,997	1,000	0,999	0,994	0,998	0,997	0,989	0,986	0,989	0,996	
PIM				0,994	0,998	0,997	0,827	0,977	0,989	0,997	
TAT				0,993	0,997	0,996	0,990	0,988	0,990	0,997	
ZCM				0,989	0,994	0,991	0,983	0,973	0,991	0,982	
AC		0,997									
VM3*					0,997						

Table 4.4: The diagonal values in the F10-UF10 correlational matrix where the columns are the acceleration preprocessing methods, the rows are the activity metrics, and each cell is the combination of the two containing the correlational value between the F10 and UF10 activity signals

4.3. Effects of bit resolution

The original data was recorded with a 12-bit resolution that, for temporal and spectral analysis, I have subsequently reduced in steps of 2 bits, meaning I ended up with 5 different acceleration signals, with 12, 10, 8, 6 and 4-bit resolution, respectively. I then determined the activity signals of the 12-bit and 8-bit accelerations using different activity calculation methods, and compared them through correlational analysis.

4.3.1. Temporal and spectral effects

The temporal representation from the same UFM acceleration with all bit values plotted onto each other can be seen in Figure 4.6. It shows, that the 12-bit (blue), 10-bit (red) and 8-bit (yellow) signals are practically indistinguishable. This implies that the differences caused by the increase in the quantization steps along the three axes is insignificant enough to get diminished. These steps go from 3,9 m*g* at 12 bits, to 15,6 m*g* at 10 bits, and to 62,5 m*g* at 8 bits. This means, that if the 12-bit value were to fall directly in the middle of the 10-bit or 8-bit steps, the maximum difference would be exactly half of the step size, so 7,8 m*g* and 31,25 m*g*, respectively. This is also known as the quantization noise. The effective value of this noise per axis can be calculated using Equation 4.1 [31]. Since this noise is present along all 3 axes, it increases in value when calculating the resultant magnitude of the acceleration signals. Equation 4.2 shows the effective value of the noise when applied to the resultant. This means, that in our case, we get that the effective value of the quantization noise is only 3,9 m*g* for the 10-bit signal and 15,63 m*g* for the 8-bit signal.

$$RMS = \frac{\Delta x}{\sqrt{12}} \tag{4.1}$$

The effective value of the quantization noise, where Δx, is half of the quantization step

$$\sqrt{\left(\frac{\Delta x}{\sqrt{12}}\right)^2 + \left(\frac{\Delta x}{\sqrt{12}}\right)^2 + \left(\frac{\Delta x}{\sqrt{12}}\right)^2} = \sqrt{3}\,\frac{\Delta x}{\sqrt{12}} \tag{4.2}$$

The effective value of the quantization noise when calculating the resultant acceleration, where Δx, is half of the quantization step

When looking at the 6-bit and 4-bit acceleration signals, we can see that these show bigger differences. The 6-bit one still somewhat follows the overall pattern, but on the other hand the 4-bit one often shows totally different behaviours. The effective value of the quantization noises in their cases are 62,5 m*g* and 250 m*g*, respectively. These values are much higher, showing that the differences get significantly bigger as the resolution is reduced more and more. At 4 bits, we only have 16 quantization values, meaning that with the range being a total of 16 *g*, the triaxial acceleration values are always an integer factor of 1. This leads to very rough estimations, and a severely distorted resulting signal.

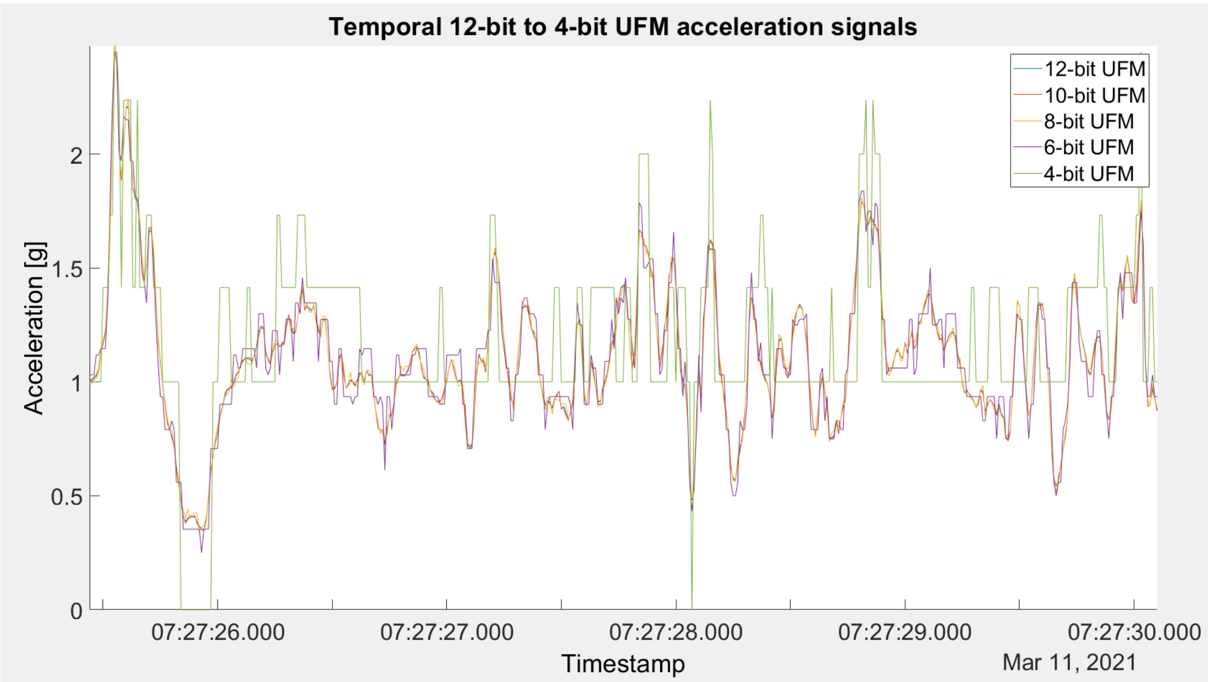

Figure 4.6: The temporal representation of the 12-bit (blue), 10-bit (red), 8-bit (yellow), 6-bit (purple) and 4-bit (green) versions of the same UFM acceleration

The spectral response of the acceleration signals shows similar results. The 10-bit and 8-bit signals are once again almost identical to the original 12-bit one. However, the 6-bit and 4-bit ones show significant elevation from these, meaning that their total power is higher than their 12-bit, 10-bit and 8-bit counterparts. This is due to the quantization noise, as well as the quantization steps being so big, that they are often roughly estimated.

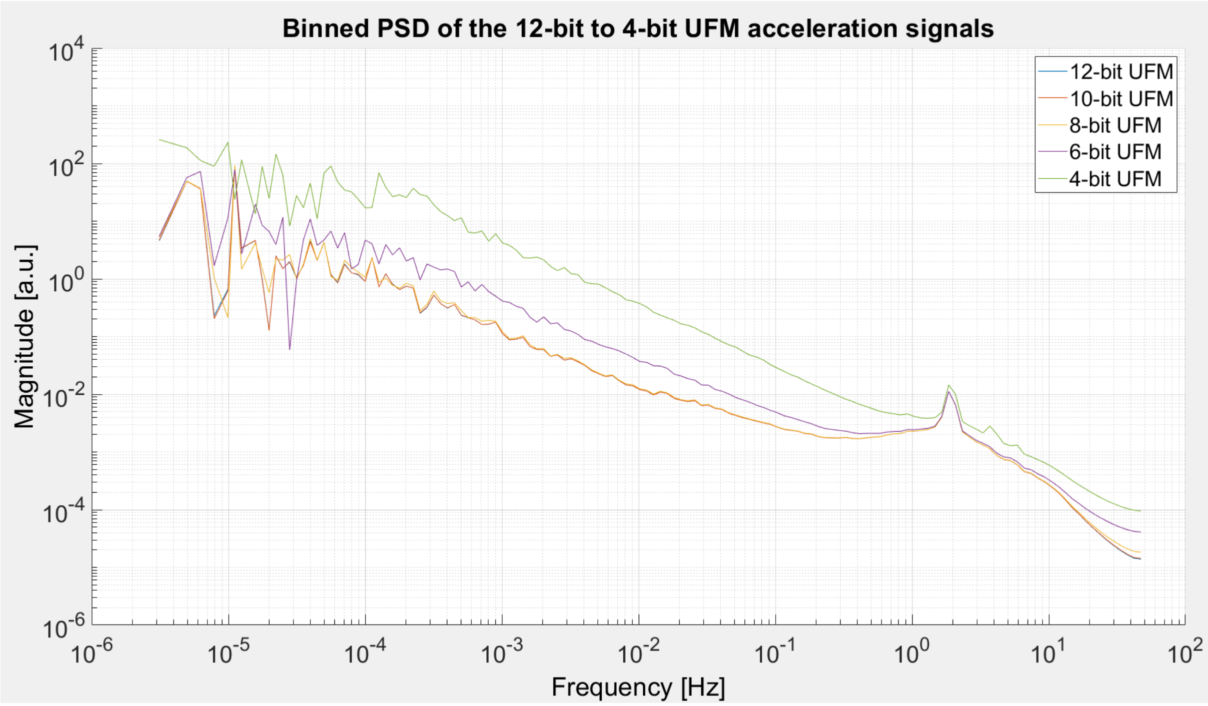

Figure 4.8: The binned power spectral density of the 12-bit (blue), 10-bit (red), 8-bit (yellow), 6-bit (purple) and 4-bit (green) versions of the same UFM acceleration

4.3.2. Correlation analysis

I calculated the correlation matrix between the set of activity signals determined from the 8-bit and 12-bit acceleration values. The resulting matrix can be seen in Figure 4.9, and their diagonal values in Table 4.5. They show similar outcomes to the other parameters. This proves, that the absolute errors the resolution reduction introduces really is negligible between the 12-bit and 8-bit signals. The diagonal values also show universally high correlation values. Even the preprocessing and metric combinations that caused some dissimilarities earlier, like PIM(UFM) or ZCM(UFM) are almost exactly 1 this time around. This implies that a full-range of 16 *g* paired with 8-bit resolution gives sufficient results. This also means that if any devices were to have smaller ranges, there is even less of a point of having higher resolution. Meanwhile, going over 16 *g* range also seems useless, as almost no human locomotor activity requires that sort of acceleration.

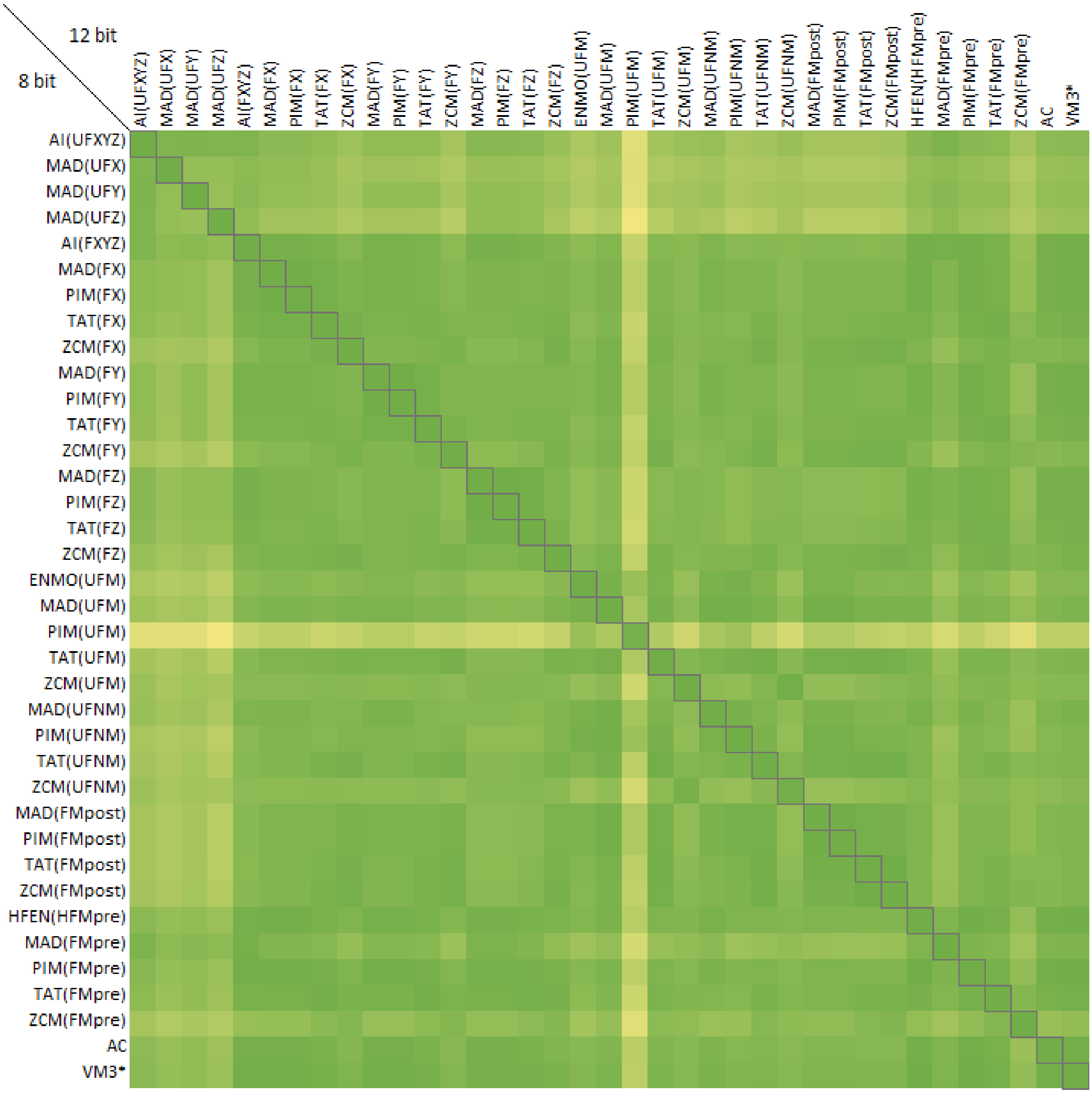

Figure 4.9: The correlational matrix between activity signals derived from 8-bit and 12-bit acceleration signals

	UFX	UFY	UFZ	FX	FY	FZ	UFM	UFNM	Fmpost	Fmpre	HFMpre
AI		1,000			1,000						
ENMO							0,994				
HFEN											0,998
MAD	0,999	0,999	0,999	1,000	1,000	1,000	0,995	0,995	1,000	1,000	
PIM				1,000	1,000	1,000	0,960	0,993	1,000	1,000	
TAT				1,000	1,000	1,000	1,000	0,998	1,000	1,000	
ZCM				0,999	1,000	0,999	0,997	0,971	1,000	0,999	
AC		1,000									
VM3*					1,000						

Table 4.5: The diagonal values in the 8bit-12bit correlational matrix where the columns are the acceleration preprocessing methods, the rows are the activity metrics, and each cell is the combination of the two containing the correlational value between the 8-bit and 12-bit activity signals

I did not make separate matrices for other resolution values, as 8 bits is already much lower than what most devices use that are out on the market [22,30]. However, for demonstrative purposes I calculated a correlation matrix from one subject's measurement that contains the correlational values between activities derived from all 5 different bit resolution acceleration signals. This matrix can be found as Figure 8.4 in the Supplementary Materials section. Unlike the others, this does not contain the AC and VM3* metrics. I want to highlight the correlation between the 12-bit and 4-bit signals shown in Figure 4.10. In this case, the pattern of the matrix clearly changes, but it is interesting, that most activity signals still show strong correlations. The diagonal values can be seen in Table 4.6, and it also displays, that other than the metrics paired with UFM or UFNM preprocessing methods the activity signals show correlational values of around 0.9. This implies, that the filters applied during certain preprocessing methods have significant impact on the activity signals.

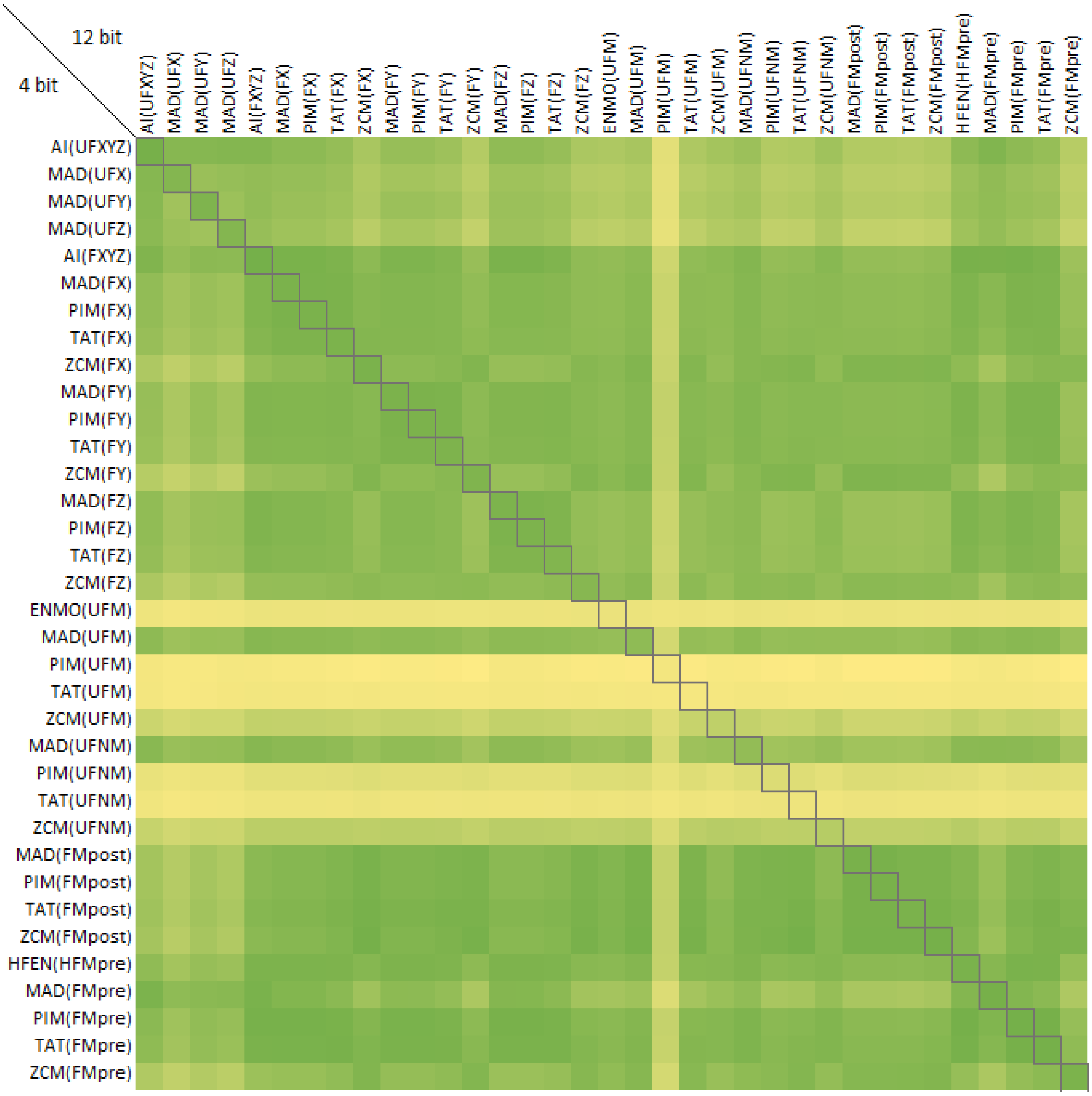

Figure 4.10: The correlational matrix between activity signals derived from 4-bit and 12-bit acceleration signals

	UFX	UFY	UFZ	FX	FY	FZ	UFM	UFNM	Fmpost	Fmpre	HFMpre
AI		0,956			0,967						
ENMO							0,146				
HFEN											0,934
MAD	0,864	0,896	0,862	0,925	0,921	0,909	0,783	0,762	0,939	0,954	
PIM				0,925	0,921	0,909	0,084	0,250	0,939	0,965	
TAT				0,918	0,905	0,879	0,077	0,123	0,928	0,959	
ZCM				0,926	0,890	0,845	0,449	0,512	0,961	0,919	

Table 4.6: The diagonal values in the 4bit-12bit correlational matrix where the columns are the acceleration preprocessing methods, the rows are the activity metrics, and each cell is the combination of the two containing the correlational value between the 4-bit and 12-bit activity signals

4.4. Case study: Effects on a manufacturer specific activity determination method

In the previous segments I concluded that neither examined parameter has any meaningful effect on the vast majority of activity signal determination methods. I wanted to further reinforce this statement by taking a look at their effects on a specific, publically available device. This is the actigraph made by the ActiGraph LLc company. I have referenced it throughout my work, and even included their activity calculation methods, namely the methods of getting Activity Counts (AC) in my correlational matrices. I suspected that since the acceleration signals go through several steps [19] before an activity is derived from them, the parameters will have little to no effect. In order to affirm this suspicion, I changed the original acceleration values by each previously examined parameter, then calculated their AC activity values. I also did this for the VM3* metric, as the research group in their previous studies suspected that this is the most similar as to how AC is calculated. With this I ended up with 5 different acceleration signals for both metrics, being the uncalibrated, calibrated, 8-bit, UF10 and F10 versions. Just like before, I then calculated the correlational values between activity signals derived from the aforementioned acceleration values and repeated the process for all 28 measurements.

The results for the AC metric are shown in Figure 4.11, and the results for the VM3* are shown in Figure 4.12. As we can see, it can be stated that the parameters have almost zero effect on the outcomes of either the Activity Count or VM3* signals. This clearly indicates, that the acceleration data collection process can be a bit more lenient at times, as they have little to no impact on the activity derived from them.

	Uncalibrated	Calibrated	8 bit	UF10	F10
Uncalibrated	1,000	1,000	1,000	0,998	1,000
Calibrated	1,000	1,000	1,000	0,998	1,000
8 bit	1,000	1,000	1,000	0,998	1,000
UF10	0,998	0,998	0,998	1,000	0,998
F10	1,000	1,000	1,000	0,998	1,000

Figure 4.11: The effects of each parameter when comparing activities calculated with the Activity Count metric

	Uncalibrated	Calibrated	8 bit	UF10	F10
Uncalibrated	1,000	1,000	1,000	0,998	1,000
Calibrated	1,000	1,000	1,000	0,998	1,000
8 bit	1,000	1,000	1,000	0,998	1,000
UF10	0,998	0,998	0,998	1,000	0,997
F10	1,000	1,000	1,000	0,997	1,000

Figure 4.12: The effects of each parameter when comparing activities calculated with the VM3* metric

5. Summary

Due to the methodology of actigraphy not being standardized, dissimilarities can appear as a direct result of determining the activity values in different ways from the same acceleration data. The research group I joined is trying to tackle this issue by highlighting these differences in the data processing steps. In the past, they collected the most commonly used activity determination methods and compared them through spectral and correlational analysis. I wanted to take a step back and examine the impact of the technical parameters of acceleration measurements on the activity signals derived from them.

Through our cooperation with sleep researchers, we received 28 different actigraphic measurements, which were recorded with 12-bit resolution and 100 Hz sampling rate. To examine the effect of changing the measurement parameters, I subsequently modified the sampling frequency to 10 Hz and reduced the bit resolution of these measurements all the way down to 4 bits, as well as applied a post-calibration algorithm that was previously made by another member of the research group. I addressed the effects of these parameters not only by examining the temporal and spectral patterns of the acceleration data but also by assessing the linear relationship between activity signals derived by numerous activity determination methods from the differently altered acceleration data through correlation-matrix-based analysis.

When examining the effects of the post-calibration algorithm, I was able to reproduce the research group's previous results on a different dataset. I was also able to determine, that the calibration has negligible effects on the correlation pattern between differently calculated activity signals.

When reducing the sampling rate of acceleration data from 100 Hz to 10 Hz, I used two different methods. The first was to simply take out every 10th data point, and – as this method can lead to aliasing –, the second approach was to apply an anti-aliasing filter before the downsampling. Then, I examined the impact of changing the sampling rate on the different activity calculation methods with correlation analysis. I found that the similarities between activity signals (i.e., the pattern of the correlation matrix) were not significantly affected by reducing the sampling frequency of the acceleration data from 100 Hz to 10 Hz. Moreover, I also showed that the aliasing effect does not cause any noteworthy discrepancies during the downsampling operation, which I demonstrated both in the time- and frequency domain.

I reduced the resolution of the acceleration signals from 12 bits down to 4 bits. When examining their temporal and spectral patterns the 10-bit and 8-bit acceleration signals showed barely any changes compared to the 12-bit signal. On the other hand, the 6-bit and 4-bit signals were affected more significantly due to the quantization noise. Through correlational analysis, I was able to show that the activity signals calculated from 8-bit acceleration data are almost identical in nature to the ones calculated from 12-bit data.

In conclusion, I found that changing the aforementioned measurement parameters has a negligible effect on the activity signals, which reinforces that possible differences between the manufacturers' solutions are not caused by the discrepancies in the technical parameters of the acceleration measurement, but rather by the different activity determination methods used in their devices. The research group plans to publish these results in the form of a journal article and the manuscript is currently being prepared. The future objectives of the presented research could be to investigate the impact of the measurement device placement (e.g., on the chest instead of the wrist) and the selection of the epoch length (e.g., 5 s instead of 1 minute).

6. References

1. Mukaka MM. A guide to appropriate use of Correlation coefficient in medical research. Malawi Medical Journal : The Journal of Medical Association of Malawi. 2012. september;24(3):69.

2. Schober P, Boer C, Schwarte LA. Correlation Coefficients: Appropriate Use and Interpretation. Anesthesia & Analgesia. 2018. may;126(5):1763.

3. Róbert M. Az 1/f-zaj időbeli szerkezete és a zajanalízis alkalmazásai. szte; 2009. https://doktori.bibl.u-szeged.hu/id/eprint/1552/

4. Using Fast Fourier Transforms and Power Spectra in LabVIEW. https://www.ni.com/en/shop/labview/using-fast-fourier-transforms-and-power-spectra-in-labview.html

5. Power Spectral Density Estimates Using FFT. [https://www.mathworks.com/help/signal/ug/power-spectral-density-estimates-using-fft.html

6. Leuenberger KD. Long-term activity and movement monitoring in neurological patients [Doctoral Thesis]. ETH Zurich; 2015 https://www.research-collection.ethz.ch/handle/20.500.11850/122013

7. Falck RS, Landry GJ, Brazendale K, Liu-Ambrose T. Measuring Physical Activity in Older Adults Using MotionWatch 8 Actigraphy: How Many Days are Needed? 2017. january 1. https://journals.humankinetics.com/view/journals/japa/25/1/article-p51.xml

8. Nakamura T, Kiyono K, Yoshiuchi K, Nakahara R, Struzik ZR, Yamamoto Y. Universal Scaling Law in Human Behavioral Organization. Phys Rev Lett. 2007. september 28.;99(13):138103.

9. Lichstein KL, Stone KC, Donaldson J, Nau SD, Soeffing JP, Murray D, Actigraphy Validation with Insomnia. Sleep. 2006. february 1.;29(2):232–9.

10. Wells ME, Overton A. Circadian Rhythm Sleep Disorders. Primary Health Care 2014;04(02). https://www.omicsgroup.org/journals/circadian-rhythm-sleep-disorders-2167-1079.1000158.pdf

11. Rezaei M, Khormali M, Akbarpour S, Sadeghniiat-Hagighi K, Shamsipour M. Sleep quality and its association with psychological distress and sleep hygiene: a cross-sectional study among pre-clinical medical students. Sleep Science. 2023. october 16.;11:274–80.

12. Faedda GL, Ohashi K, Hernandez M, McGreenery CE, Grant MC, Baroni A. Actigraph measures discriminate pediatric bipolar disorder from attention-deficit/hyperactivity disorder

and typically developing controls. Journal of Child Psychology and Psychiatry. 2016;57(6):706–16.

13. Migueles JH, Cadenas-Sanchez C, Ekelund U, Delisle Nyström C, Mora-Gonzalez J, Löf M. Accelerometer Data Collection and Processing Criteria to Assess Physical Activity and Other Outcomes: A Systematic Review and Practical Considerations. Sports Med. 2017. september 1.;47(9):1821–45.

14. Ancoli-Israel S, Cole R, Alessi C, Chambers M, Moorcroft W, Pollak CP. The Role of Actigraphy in the Study of Sleep and Circadian Rhythms. Sleep. 2003. may 1.;26(3):342–92.

15. Meltzer LJ, Montgomery-Downs HE, Insana SP, Walsh CM. Use of actigraphy for assessment in pediatric sleep research. Sleep Medicine Reviews. 2012. october 1.;16(5):463–75.

16. Maczák B, Vadai G, Dér A, Szendi I, Gingl Z. Detailed analysis and comparison of different activity metrics. PLOS ONE. 2021. december 21.;16(12):e0261718.

17. Maczák B, Gingl Z, Vadai G. General spectral characteristics of human activity and its inherent scale-free fluctuations. Sci Rep. 2024. january 31.;14(1):2604.

18. Brønd JC, Andersen LB, Arvidsson D. Generating ActiGraph Counts from Raw Acceleration Recorded by an Alternative Monitor. Medicine & Science in Sports & Exercise. 2017. 0;49(11):2351.

19. Neishabouri A, Nguyen J, Samuelsson J, Guthrie T, Biggs M, Wyatt J. Quantification of acceleration as activity counts in ActiGraph wearable. Sci Rep. 2022. july 13.;12(1):11958.

20. Axivity | Help Article https://axivity.com/help/18

21. Duncan S, Stewart T, Schneller MB, Godbole S, Cain K, Kerr J. Convergent validity of ActiGraph and Actical accelerometers for estimating physical activity in adults. PLOS ONE. 2018. june 12.;13(6):e0198587.

22. Esmaeilzadeh S. Fibion. 2024. GENEActiv Specifications. https://web.fibion.com/articles/geneactiv-specifications/

23. Farago D, Maczak B, Gingl Z. Enhancing Accuracy in Actigraphic Measurements: A Lightweight Calibration Method for Triaxial Accelerometers. IEEE Access. 2024;12:38102–11.

24. What is downsampling? | IBM 2024https://www.ibm.com/topics/downsampling

25. WolfSound What is aliasing? What causes it? How to avoid it? https://thewolfsound.com/what-is-aliasing-what-causes-it-how-to-avoid-it/

26. DigiKey. The Basics of Anti-Aliasing Low-Pass Filters (and Why They Need to be Matched to the ADC). https://www.digikey.com.br/pt/articles/the-basics-of-anti-aliasing-low-pass-filters

27. decimate https://www.mathworks.com/help/signal/ref/decimate.html

28. PAL family https://www.palt.com/pals/

29. AX3 http://www.axivity.com/product/1

30. Esmaeilzadeh S. Fibion. 2024. ActiGraph GT3X Specifications. https://web.fibion.com/articles/actigraph-gt3x-specifications/

31. Quantization Noise - an overview | ScienceDirect Topics https://www.sciencedirect.com/topics/computer-science/quantization-noise

7. Acknowledgement

I would like to express my appreciation to Dr. Zoltán Gingl, head of the Department of Technical Informatics for his insightful ideas throughout my work.
I am grateful to Dr. Róbert Bódizs and G. Csenge Horváth, sleep researchers at Semmelweis University, Institute of Behavioural Sciences for providing the necessary measurements for my analysis.
Special thanks to my supervisors, Dr. Gergely Vadai, assistant professor and Bálint Maczák PhD student, for helping me throughout my work.

8. Supplementary materials

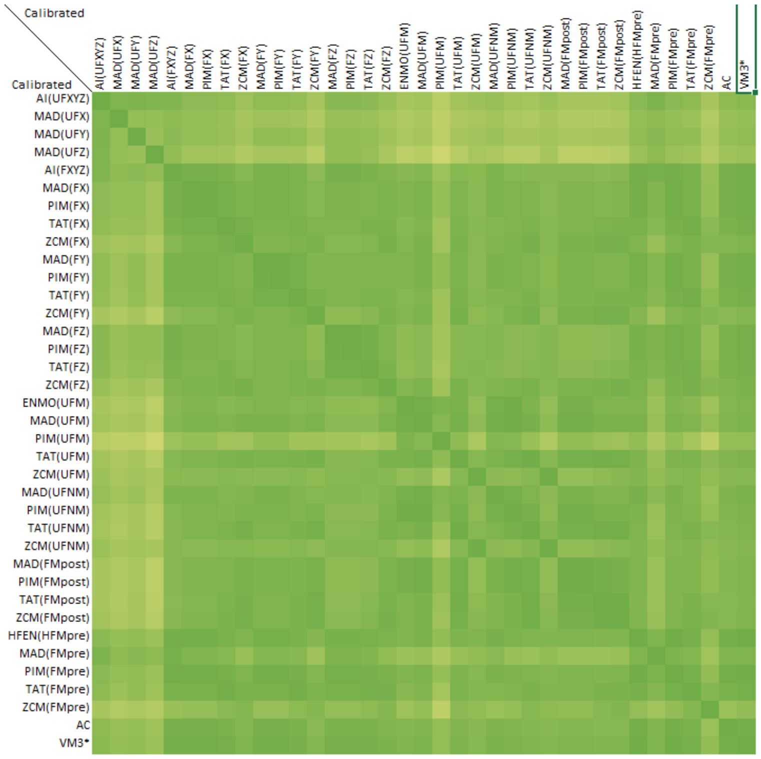

Figure 8.1: The correlational matrix between activity signals derived from calibrated-calibrated acceleration signals

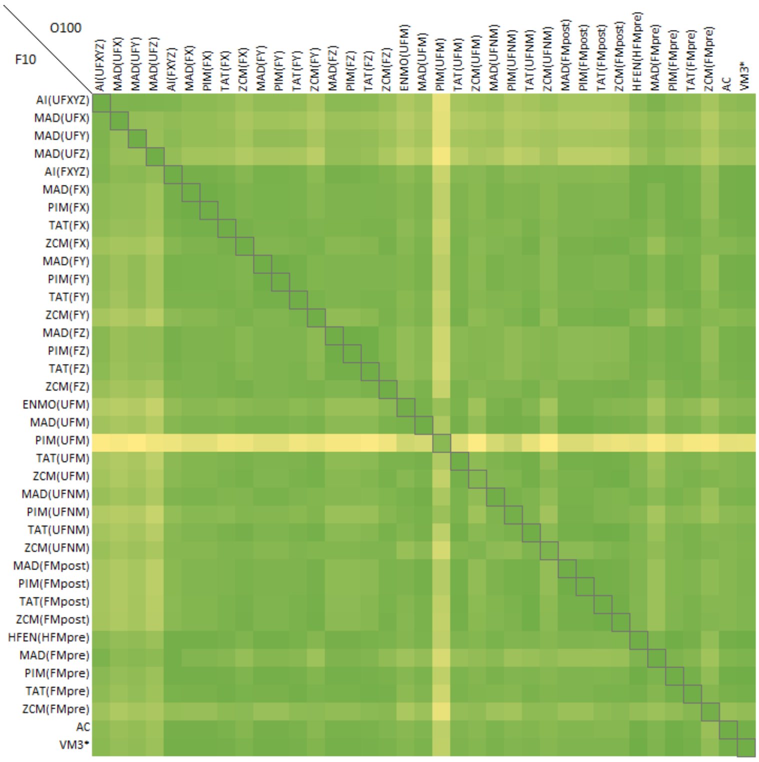

Figure 8.2: The correlational matrix between activity signals derived from F10 and O100 acceleration signals

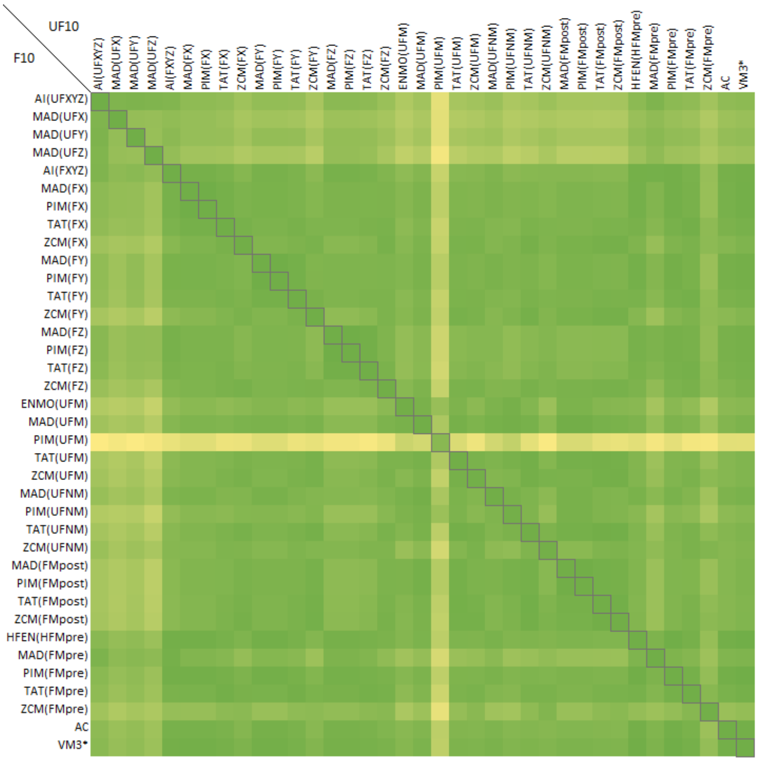

Figure 8.3: The correlational matrix between activity signals derived from F10 and UF10 acceleration signals

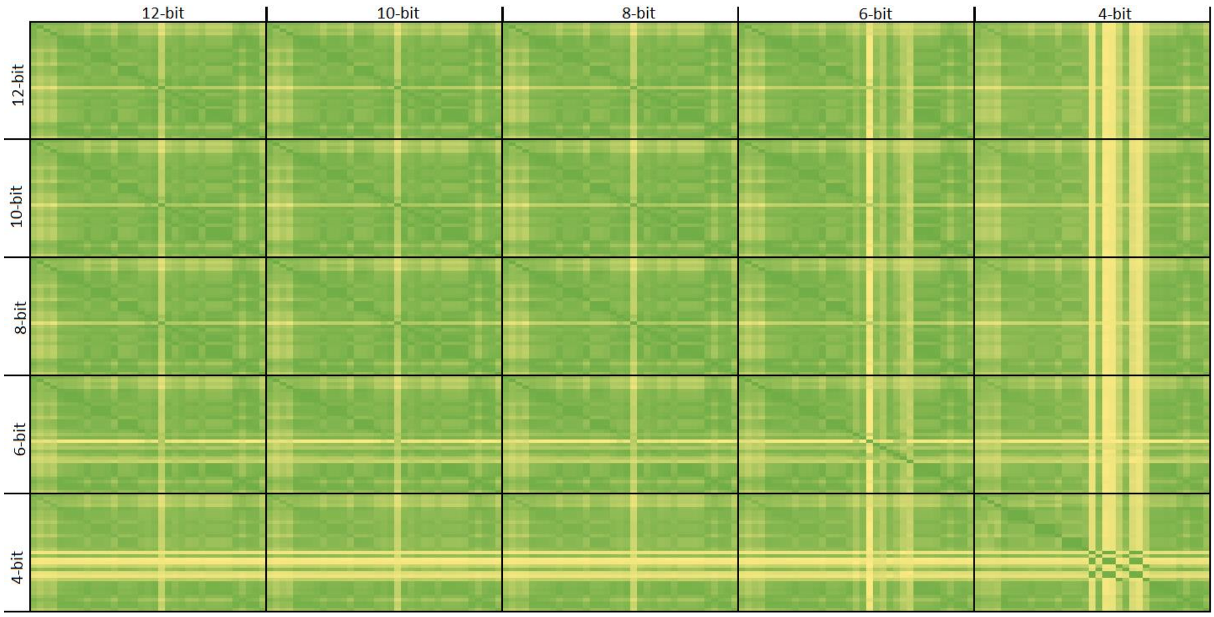

Figure 8.4: The correlational matrix between activity signals derived from 12-bit, 10-bit, 8-bit, 6-bit and 4-bit acceleration signals